Carbohydrate Polymers 86 (2011) 1445–1450

Contents lists available at ScienceDirect

Carbohydrate Polymers

journal homepage: www.elsevier.com/locate/carbpol

TEMPO-mediated oxidation of lignocellulosic fibers from date palm leaves

Adil Sbiai[a,b,c,d], Hamid Kaddami[d,*], Henry Sautereau[a,b,c], Abderrahim Maazouz[a,b,c], Etienne Fleury[a,b,c]

[a] Université de Lyon, Lyon F-69003, France
[b] INSA de Lyon, IMP/LMM Laboratoire des Matériaux Macromoléculaires, Villeurbanne F-69621, France
[c] CNRS, UMR 5223, Ingénierie des Matériaux Polymères, Villeurbanne F-69621, France
[d] Université Cadi Ayyad, Laboratoire de Chimie Bioorganique et Macromoléculaire, Faculté des Sciences et Techniques Guéliz, Avenue Abdelkrim Khattabi BP 549, 40000 Marrakech, Morocco

ARTICLE INFO

Article history:
Received 30 March 2011
Received in revised form 23 May 2011
Accepted 4 June 2011
Available online 30 June 2011

Keywords:
TEMPO
Selective oxidation
Cellulose
Lignocellulosic fibers
Date palm
Kinetics

ABSTRACT

The TEMPO-mediated oxidation of date palm lignocellulosic fibers (DPLF) from *Phoenix dactylifera* – i.e. cellulosic fibers still containing their initial lignin and hemicellulose components – was performed under conditions leading to a high degree of oxidation. The resulting carboxylated fibers were shown to still contain high residual contents of lignin (12%, w/w) and hemicelluloses (34%, w/w). The ultrastructure of the oxidized DPLF was revealed by scanning electron microscopy, energy dispersive X-ray and X-ray photoelectron spectroscopy. These techniques not only confirmed the surface carboxylation of the DPLF, but also gave some insight on the oxidation heterogeneity when going from the surface to the core of the fibers. Finally, in relation with the chemical data and the morphology of the substrate, it has been possible to propose a heterogeneous oxidation kinetic model, which was applied with success not only to DPLF but also to the cellulose whiskers extracted from the rachis of the palm from *P. dactylifera*.

1. Introduction

Owing to their renewable character combined with their low cost and abundance, lignocellulosic fibers extracted from wood and annual plants have received growing attention as an alternative to glass fibers in composite processing. Indeed the use of such natural product for the reinforcement of thermoplastic or thermosetting resins, leads to composites with lower density, higher specific stiffness and strength, together with a better biodegradability (Bledzki & Gassan, 1999; Gandini, 2008; Mishra, Mohanty, Drzal, Misra, & Hinrichsen, 2004; Zimmermann, Pöhler, & Geiger, 2004). The mechanical properties of these bio-based composites are directly related to the nature of the fiber/matrix interface where a maximum of adhesion is required to render possible the transfer of mechanical constraints to the fiber when a load is applied to the composite.

In most cases, the hydrophilic nature of the lignocellulosic fibers is detrimental for their interface interactions with common resins, which are mostly hydrophobic. Thus, chemical treatments have to be applied to overcome this issue (Reich, El Sabbagh, & Steuernagel, 2008). For this purpose, various surface modifications have been devised to selectively replace hydroxyl functions with hydrophobic groups (Biagiotti et al., 2004; Duanmu, Gamstedt, & Rosling, 2007; Gandini, 2008; Goussé, Chanzy, Cerrada, & Fleury, 2004). Coupling agents giving rise to covalent junctions between the fibers and the matrix have also been described (Abdelmouleh et al., 2002; Bendahou et al., 2008; González-Sánchez, González-Quesada, De La Orden, & Urreaga, 2008; Paunikallio, Suvanto, & Pakkanen, 2006).

In a few instances, an enhanced polar modification of the fiber surfaces is desired to accommodate polymer matrices such as polyphenol (Li, Renneckar, & Barone, 2010) or polyepoxy. For epoxy composites prepared by Resin Transfert Molding, the consequences were thus the improvement of the process and the increase of mechanical properties as obtained from high strain tests (Sbiai, Maazouz, Fleury, Sautereau, & Kaddami, 2010).

Such modifications are usually achieved by converting some of the surface OH moieties of cellulose into carboxyl groups, which promote the interaction of the fibers with the resins in question. At present, the catalytic oxidation using 2,2,6,6-tetramethylpiperidine-1-oxyl (TEMPO) radical under mild aqueous conditions was found to be the most straightforward and efficient method to selectively oxidize hydroxyl functions located at the surface of cellulosic fibers and to convert them into sodium carboxylate (Okita, Saito, & Isogai, 2010). This method has been widely used on various kinds of well defined purified cellulose substrates: cotton linters (Saito & Isogai, 2004), cellulose microfibrils from sugar beet (Montanari, Roumani, Heux, & Vignon, 2005), tunicin whiskers (Habibi, Chanzy, & Vignon, 2006), bleached hardwood kraft pulp

---

* Corresponding author. Tel.: +212 661071386; fax: +212 524433170.
E-mail address: hkaddami@yahoo.fr (H. Kaddami).

0144-8617/$ – see front matter © 2011 Elsevier Ltd. All rights reserved.
doi:10.1016/j.carbpol.2011.06.005

(Saito et al., 2009), bleached softwood kraft pulps (Dang, Zhang, & Ragauskas, 2007), fibrillated viscose rayon fibers (Shibata & Isogai, 2003), and even water soluble cellulose acetate (Gomez-Bujedo, Fleury, & Vignon, 2004) etc. . .

Our present work is devoted to the TEMPO-mediated oxidation of lignocellulosic fibers isolated from the leaflets of date palm (*Phoenix dactylifera* L.), a plant largely unexploited despite significant amounts of waste annually available (Kaddami et al., 2006). To our knowledge, the surface oxidation of such raw substrates has not been investigated in depth so far, as we note only a few reports dealing only with the oxidation of thermomechanical pulp (Okita, Saito, & Isogai, 2009; Han, Law, Daneault, & Lanouette, 2008; Mao, Law, Daneault, & Brouillette, 2008). Herein, we describe the effect of the TEMPO-mediated oxidation on the chemical composition (lignin, hemicellulose and cellulose) and on the shape of the date palm lignocellulosic fibers (DPLF). The kinetic aspect was also investigated with a model taking into account the heterogeneous character of the reaction.

2. Experimental

2.1. Materials

Leaflets from palm leaves of *P. dactylifera* were cut into pieces with lengths of 3–5 cm. After 24 h soxhlet extraction with acetone/ethanol (75/25 by vol), the resulting product was slightly discolored. It was then ground and sieved in order to eliminate the fine powder and to keep only the particles with length ranging from 2 to 10 mm and widths from 0.2 to 0.8 mm. This material is hereafter called lignocellulosic fibers from date palm leaflets or DPLF. For XRD analysis, the samples were ground again to obtain a fine powder.

Cellulose, lignin and hemicellulose were extracted from the DPLF according to a previously described procedure (Bendahou, Dufresne, Kaddami, & Habibi, 2007). Cellulose whiskers were prepared from the rachis of *P. dactylifera* leaves (Bendahou, Habibi, Kaddami, & Dufresne, 2009).

2,2,6,6-Tetramethylpiperidine-1-oxyl radical (TEMPO), sodium bromide, and 10% sodium hypochlorite solution were purchased from Sigma–Aldrich and used as received.

2.2. General procedure for oxidative treatment (Gomez-Bujedo et al., 2004)

2 g of DPLF were stirred in 200 mL distilled water for 1 min. TEMPO (32 mg, 0.065 mmol) and NaBr (0.636 g, 1.9 mmol) were dissolved in the suspension maintained at 4 °C. TEMPO-mediated oxidation was initiated by adding dropwise the sodium hypochlorite solution (10%, 32 mL, 43 mmol) and adjusting the pH at 10 by addition of a 0.1 M aqueous HCl. The suspension was then maintained at pH 10 ± 0.5 by continuous addition of 0.5 M NaOH and at 4 °C by means of a thermo-controlled bath. When the pH became stable, the reaction was quenched by adding methanol (5 mL). After neutralization of the reaction mixture to pH 7 by addition of 0.1 M HCl, the suspension was filtrated and the solid particles were washed with distilled water and dried under vacuum at 30 °C for 18 h. The soluble part was freeze-dried.

The same oxidation procedure was applied to the other samples, namely the cellulose, the hemicellulose and the lignin extracted from the DPLF, together with the cellulose whiskers extracted from the leave rachis.

2.3. Analysis techniques

The composition of the DPLF before and after oxidation i.e. the weight fraction of their cellulose, hemicellulose, and lignin contents was determined by selective extraction according to the NF T12-011 standard.

The carboxylate content of oxidized cellulose samples was determined by conductometric titrations (Saito & Isogai, 2004).

Infrared spectra were recorded on a FT-IR Perkin-Elmer 1720X spectrometer collecting 20 scans from 400 to 4000 cm^{-1}. Oxidized DPLF was converted to its acid form by ion exchange in order to displace the carboxyl absorption band toward higher wavelengths, thus eliminating any interference with the absorbed water band at 1640 cm^{-1}. Consequently the superposition of the sodium carboxylate peak with those of the hydrogen bonds could be avoided. The samples were dried with acetone and analyzed as KBr.

Solid-state ^{13}C NMR spectra were recorded on a Bruker DSX 300 spectrometer fitted with a 4 mm CP/MAS probe. The experiments were run overnight (c.a. 25 000 scans) using the CP/MAS technique, with a 2 ms contact time and a 2 s recycle delay to allow a complete proton relaxation. Proton decoupling was achieved using the TPPI method, with an 83 kHz rf field.

The XPS spectra were measured using an AXIS ULTRA DLD X-ray photoelectron spectrometer (KRATOS ANALYTICAL). Samples were dried at 50 °C under vacuum during 24 h, and set with conductive carbon adhesive tabs. The measurements were performed using a monochromatic Al Kα X-ray with a pass energy of 160 eV and a coaxial charge neutralizer. The base pressure in the analysis chamber was smaller than 5×10^{-8} Pa. XPS spectra of O1s and C1s levels were measured at a normal angle with respect to the plane of the surface. High resolution spectra were corrected for charging effects by assigning a value of 284.6 eV to the C1s peak (adventitious carbon). Binding energies were determined with an accuracy of ±0.2 eV. The spectral decomposition of the C1s and O1s photoelectron peaks was carried out using a Shirley background at positions and FWHMs corresponding to known components, applying a 30% Lorentzian-to-Gaussian peak shape ratio.

The distribution of sodium and calcium ions present in a cross-section of the TEMPO-oxidized fibers was evaluated by the line analysis mode using an energy dispersive X-ray (EDX) device fitted into a scanning electron microscope (SEM) (Hitachi S3500N). The X-ray detector was a Thermo Noran Superdry II having a resolution of 143 eV. The analyses were performed without prior metallization of the samples.

A Philips X'Pert diffractometer equipped with a ceramic X-ray diffraction tube operated at 40 kV and 40 mA with Cu Kα radiation (wavelength 0.15418 nm) was used to determine the crystalline index of the specimens. The samples were compressed into disks using a cylindrical steel mould (Ø = 15 mm) with an applied pressure of 32 MPa. The diffracted intensity was recorded for 2θ angles in the range of 10–40°. Data were treated according to the empirical Segal method (Segal, Creely, Martin, & Conrad, 1959).

3. Results and discussion

3.1. TEMPO-mediated oxidation

DPLF samples were oxidized with TEMPO in aqueous medium. The experiments were performed (i) at low temperature (4 °C) to avoid the formation of side products and (ii) in the presence of a large quantity of sodium hypochlorite, i.e., 21 mmol/g of the DPLF, in order to reach a high degree of oxidation (Montanari et al., 2005; Okita et al., 2009). The selective oxidation of a hydroxymethyl group to a carboxyl via an aldehyde requires two moles of NaOCl per mole of hydroxyl according to the known TEMPO mechanism (Fig. 1) (De Nooy, Besemer, & van Bekkum, 1995). The kinetic of the reaction was directly followed by addition of an aqueous NaOH solution which neutralizes the carboxylic acid functions resulting from the oxidation. Fig. 2 clearly illustrates the efficiency of the reaction

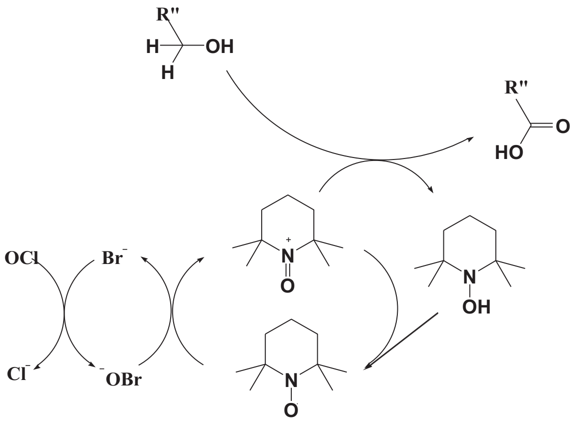

Fig. 1. Scheme of the catalytic cycle for the oxidation of a primary hydroxyl.

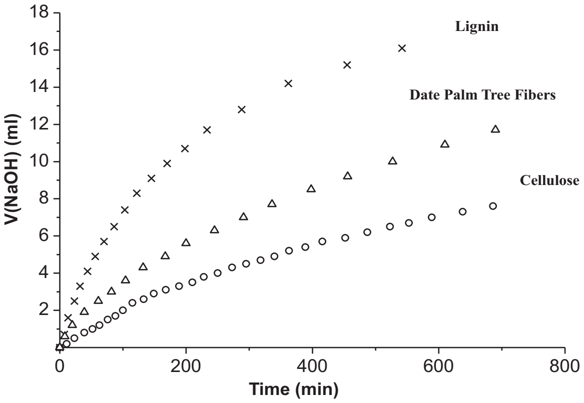

Fig. 2. Kinetic TEMPO-mediated oxidation of DPLF, the extracted cellulose and lignin from DPLF: consumption of the NaOH with the reaction time.

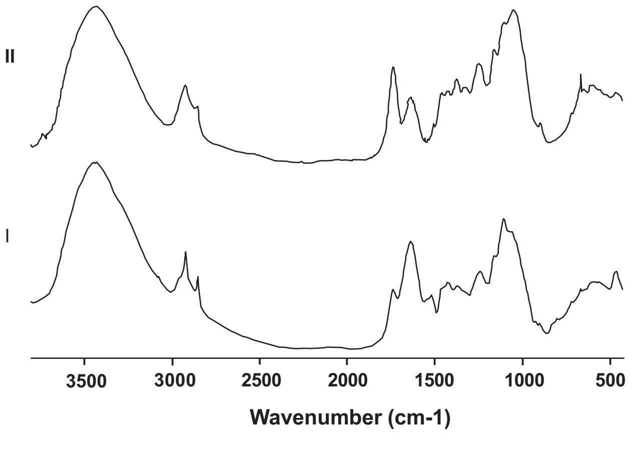

Fig. 3. FT-IR spectra for DPLF before (I) and after TEMPO-mediated oxidation (II).

with a continuous increase in NaOH consumption over a period of 720 min. According to FTIR analysis on the water insoluble fraction (Fig. 3), a stretching vibration C═O from the free COOH band near 1737 cm^{-1} was seen to have a higher intensity in the case of oxidized fibers as opposed to their non-oxidized counterparts, thus providing evidence of the oxidation. Finally, as expected, the degree of oxidation (*Do*) was found to be 0.71 ± 0.02 (Table 1).

The composition of DPLF was also investigated since a significant amount (30%) of the material became soluble in water during the oxidation. The results presented in Table 1 show that the proportions between components of DPLF have changed before and after the chemical oxidative treatment. Thus cellulose content has increased from 35 to 46%, whereas lignin and hemicelluloses contents have decreased. Nevertheless both lignin and hemicelluloses were still present in the oxidized DPLF at high concentration respectively 12 and 34 wt%. Okita et al. have reported on a complete elimination of lignin and hemicelluloses in the case of TEMPO-mediated oxidation of thermomechanical softwood pulp under similar processing conditions (Okita et al., 2009). Pulp used by these authors contained similar percentage of lignin and hemicelluloses but was pried open by the mechanical refining process. One can thus deduce that thermomechanical pulps are much more reactive than lignocellulosic fibers having undergone no activation. On the other hand, a weak increase of the crystalline index is observed. This could be explained by the dissolution of the lignin after oxidation. Actually, this dissolution would induce a weak decrease of the intensity of the amorphous peak I_{am} at $2\theta = 18^\circ$ (Table 1 and supporting info S1).

In order to compare the reactivity toward oxidation of each component of the DPLF, cellulose, hemicelluloses and lignin were extracted and subjected to the oxidation procedure. Kinetic data were recorded, except for hemicelluloses which presented very fast and uncontrollable kinetic. Data illustrated in Fig. 2 clearly show that the extracted lignin reacted faster than the extracted cellulose, whereas the DPLF presented an intermediate rate. The structural characterization of the oxidized lignin and hemicellulose was not undertaken due to the complexity of possible structures. However, a previous study has shown that hemicelluloses extracted from the leaflets and rachis of the *P. dactylifera* palm consist of arabinoglucuronoxylans, which are either soluble or insoluble in hot water depending on the molar content of 4-O-methyl-glucuronic acid (Bendahou et al., 2007). One can thus deduce that the oxidative treatment under aqueous conditions allowed the conversion of the hydroxymethyl group of the arabinose moieties into carboxylic functions, which further facilitated the hemicellulose extraction in reaction medium maintained at 4 °C. For lignin, the conversion of primary hydroxyl functions led to hydrosoluble products as already described (Okita et al., 2009).

The reason for the moderate reactivity of the cellulose was already described. It originates from the crystalline nature of cellulose and from the difficulty to access to the hydroxyl groups at the surface of the cellulose crystals. In contrast, lignin and hemicelluloses, which are amorphous, react faster. The TEMPO-mediated oxidation of the cellulose sample was confirmed by the appearance of the characteristic carboxylic signal at 176 ppm in the ^{13}C CP-MAS NMR spectrum (Martins, Forato, Mattoso, & Colnago, 2006; Wikberg & Maunu, 2004) corresponding to a degree of oxidation (*Do*) equal to 0.07 (See supporting info S2 and S3).

3.2. *Heterogeneous kinetic modeling*

Only few kinetic studies of TEMPO-mediated selective oxidation of cellulosic material have been reported in the literature (De Nooy

Table 1
Chemical characterization of DPLF before and after TEMPO-mediated oxidation.

Samples	[COOH] mmol/g	Crystalline index %	Composition cellulose/hemicellulose/lignin %	Water insoluble fraction %
Control DPLF	0	49.5 ± 0.5	35/28/27	100
Oxidized DPLF	0.71	52.5 ± 0.5	46/34/12	70

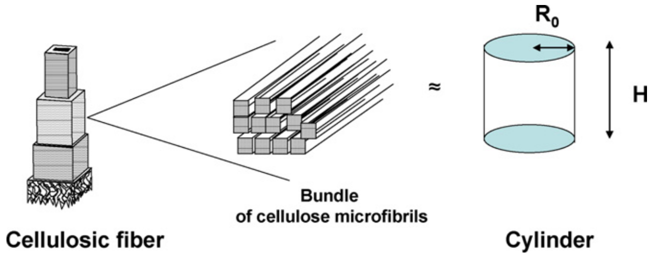

Fig. 4. Schematization of the reactive substrate presented as a cylinder.

et al., 1995; Sun et al., 2005; Mao, Ma, Law, Daneault, & Brouillette, 2010). The authors have observed a first-order kinetic with respect to TEMPO and NaBr as well as a rate constant determined by their concentrations. It has also been claimed that the NaOCl concentration affects mainly the level of the conversion, leading to the possibility of reusing the reaction liquid by addition of more NaOCl. However, although TEMPO-mediated oxidation of cellulose corresponds to a reaction between a solid phase and a liquid phase, the heterogeneous aspect of the reaction was never envisaged.

In fact, cellulose fibers can be represented as accessible porous networks, where reagents can diffuse to the periphery of entities made up of bundles of cellulose microfibrils surrounded with lignin and/or hemicelluloses. This system can be described as a cylinder (Fig. 4) with a diameter that becomes decreased when the TEMPO-mediated oxidative process progresses.

The interfacial specific rate r_{is} of an heterogeneous reaction can be expressed by Eq. (1) where R and H are respectively the radius and the height of the cylinder and k the rate constant for a given temperature and concentration (Levenspiel, 1972):

$$r_{\mathrm{is}} = 2\pi RHk \tag{1}$$

Considering R_0 as the initial radius, the conversion of the reaction at time t, is given by

$$X = \frac{R_0^2 - R^2}{R_0^2} \tag{2}$$

Since the initial molar concentration of the reactive function is n_0, its decrease with time can be described by Eq. (3):

$$dn = 2\pi RHr_{\mathrm{is}}\,dt = n_0 dX = -\frac{2n_0}{{R_0}^2} R\,dR \tag{3}$$

where

$$dX = d\left(\frac{{R_0}^2 - R^2}{{R_0}^2}\right)$$

Eq. (3) can be simplified into:

$$dn = 2\pi Hr_{\mathrm{is}}\,dt = -\left(\frac{2n_0}{{R_0}^2}\right)\,dR$$

which, after integration, gives the following relation:

$$R = R_0 - \frac{\pi H{R_0}^2 r_{\mathrm{is}}}{n_0} t \tag{4}$$

By expressing the time required for a complete conversion to occurs as:

$$t_{\mathrm{Final}} = \frac{n_0}{\pi HR_0 r_{\mathrm{is}}}$$

and rearranging the relation, one obtains:

$$(1 - X)^{1/2} = 1 - \frac{t}{t_{\mathrm{Final}}} \tag{5}$$

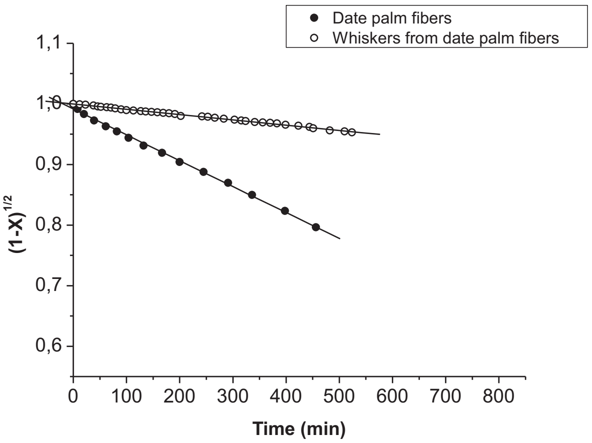

Fig. 5. Modeling of the kinetics of TEMPO-mediated oxidation for (♦) DPLF: $(1 - X)^{1/2} = 1 - 4.93 \times 10^{-4}$ t and (◯) cellulose whiskers from data palm rachis: $(1 - X)^{1/2} = 1 - 8.71 \times 10^{-5}$ t.

The conversion X was calculated from the evolution of the NaOH consumption given in Fig. 2 and the evolution of $(1 - X)^{1/2}$ was plotted as a function of t. The results are presented in Fig. 5, and as illustrated, the experimental values followed a linear equation as

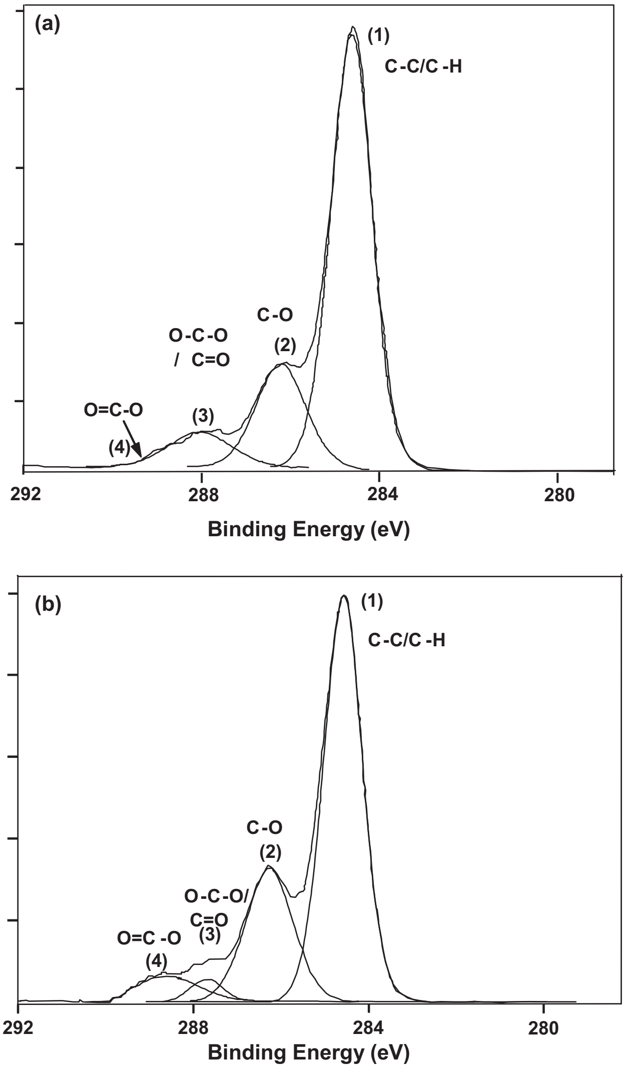

Fig. 6. High resolution C1s spectra for DPLF (a) and after (b) TEMPO-mediated oxidation.

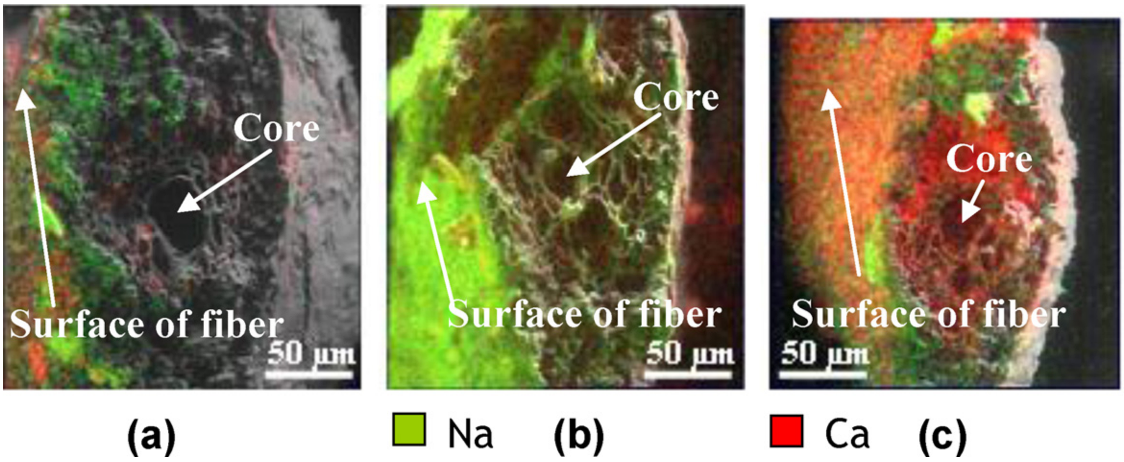

Fig. 7. Energy dispersive X-ray analysis on fiber cross-section (a) before oxidation, (b) after oxidation, and (c) after oxidation and ion-exchanged with $CaCl_2$. The colored parts correspond to the presence of the counter-ion of the carboxylate function: sodium in case of (a) and (b) and calcium in case of (c). (For interpretation of the references to color in this figure legend, the reader is referred to the web version of the article.)

predicted by the model. The value of t_{Final} calculated from the slope of the curves was 11×10^3 min.

Additional experiments were attempted, using cellulose whiskers extracted from the rachis of the from *P. dactylifera* palm. Here, the advantage was to have a pure cellulose substrate with a known length and a squarish cross-section. Consequently, the shape of the cellulose whiskers could be modeled as that of a cylinder (Elazzouzi-Hafraoui et al., 2008). The results presented in Fig. 5 are also compatible with a heterogeneous model and clearly highlight that cellulose whiskers behave in a manner analogous to that of DPLF. However for the whiskers, the t_{Final} was higher (1.1×10^4 min) than for DPLF which caused the specific rate r_{is} of the TEMPO-mediated oxidation to decrease. The difference can be ascribed to high reactivity of DPLF which contain lignin, hemicelluloses and amorphous cellulose being more reactive than cellulose whiskers.

3.3. *Topological characterization*

From the aforementioned model it can be inferred that the oxidation reaction occurs through a heterogeneous process. To characterize the topology of the chemical changes, X-rays photoelectron spectroscopy (XPS) and energy dispersive X-rays analysis were carried out on DPLF before and after oxidative treatment.

XPS revealed the modifications resulting from the oxidation (Fig. 6). Indeed the C1s spectrum of the control product (spectrum a) consists of three major peaks at 284.6 eV (peak 1), 286.2 eV (peak 2) and 287.8 eV (peak 3), corresponding to C–C + C–H, C–O and O–C–O (and/or C=O) groups respectively. After oxidation (spectrum b), a new peak can be clearly distinguished at 288.8 eV and is attributed to the O=C–O function, typical of carboxylate group. This signal is overlapped with the one of the C=O group and is probably also present in the C1 spectrum of the control product but at lower level. In addition, a quantitative analysis indicates that the atomic concentration of non-oxidized carbon (peak 1) is of 71.2% and 64.4% before and after oxidation respectively. Assuming that XPS analysis only characterize a depth of 10 nm, these results clearly highlight that carboxylate functions are present at the top layers of DPLF.

The location of carboxylate groups was clearly evidenced by the characterization with SEM/EDX analysis. In Fig. 7 are represented typical cross-sections of DPLF showing also the external wall of the fibers before oxidation (Fig. 7a), after oxidation (Fig. 7b) and after oxidation and calcium ions exchange (Fig. 7c). Zones which are colored correspond to the location of the counter-ion of carboxylate functions. The more intense the coloration, the higher is the concentration of the counter-ion and therefore the carboxylate function.

Fig. 7a shows the DPLF before oxidation and the coloration represents the mapping of sodium ions due to the presence of 4-O-methyl-glucuronic acid units within the raw fibers as mentioned above. The density of initial carboxylate is low in comparison to the one observed in the case of oxidized fibers (Fig. 7b) indicating the success of the oxidation treatment. TEMPO-oxidized fibers treated within an aqueous calcium chloride solution led to fibers-$COOCa^+$ structures (Saito, Shibata, Isogai, Suguri, & Sumikawa, 2005). As shown in Fig. 7c, the density of calcium ion is high and comparable to that obtained with sodium.

It can also be noted that carboxylate groups are found to be slightly more dense at the surface of the fibers than inside, whereas the distribution at the surface is homogeneous and the one inside inhomogeneous. Such difference between the core and the surface which is confirmed with both mapping of calcium and sodium ions was never reported before.

This feature may be ascribed to the presence of hemicelluloses and lignin, which either limit the diffusion of the reagent within the fibers or – which is more probable – migrate to the surfaces after being oxidized. It is also important to underline that the morphology of the fibers remains identical after the TEMPO mediated-oxidation as shown in Fig. 7.

4. Conclusion

The results presented in this study show that date palm lignocellulosic fibers with high lignin and hemicelluloses contents have been successively modified by a classical TEMPO-mediated oxidation process.

Despite the composite character of the fibers substrate, kinetic results have proved that oxidation has occurred in a heterogeneous manner. In contrast to previous studies, it was possible to perform this efficient and aqueous chemoselective reaction without destruction of the fibers structure, while keeping a large amount of residual lignin and hemicelluloses. It was further demonstrated that the distribution of the carboxylate group was unconventional, with an inhomogeneity between the core and the surface of the fibers probably due to a migration of the oxidized and partially hydrosoluble product.

The TEMPO-mediated oxidation of lignocellulosic fibers, as described herein, open the way for their utilization as fillers within an epoxy matrix or other matrix capable of reacting with carboxylic functions.

Acknowledgments

The authors thank for their financial support the Hassan II Academy of Sciences and Engineering and the French Ministry of Foreign Affairs (Corus program 6046). The authors also thank H. Chanzy for valuable discussions.

Appendix A. Supplementary data

Supplementary data associated with this article can be found, in the online version, at doi:10.1016/j.carbpol.2011.06.005.

References

Abdelmouleh, M., Boufi, S., Salah, B. A., Belgacem, M., Naceur, M. N., & Gandini, A. (2002). Interaction of silane coupling agents with cellulose. *Langmuir*, *18*, 3203–3208.

Bendahou, A., Dufresne, A., Kaddami, H., & Habibi, Y. (2007). Isolation and structural characterization of hemicelluloses from palm of *Phoenix dactylifera* L. *Carbohydrate Polymers*, *68*, 601–608.

Bendahou, A., Kaddami, H., Sautereau, H., Raihane, M., Erchiqui, F., & Dufresne, A. (2008). Short palm tree fibers poly olefin composites: Effect of filler content and coupling agent on physical properties. *Macromolecular Materials and Engineering*, *293*, 140–148.

Bendahou, A., Habibi, Y., Kaddami, H., & Dufresne, A. (2009). Physico-chemical characterization of palm from *Phoenix dactylifera*-L., preparation of cellulose whiskers and natural rubber-based nanocomposites. *Journal of Biobased Materials and Bioenergy*, *3*, 81–90.

Biagiotti, J., Puglia, D., Torre, L., Kenny, J. M., Arbelaiz, A., Marieta, C., et al. (2004). A systematic investigation on the influence of the chemical treatment of natural fibers on the properties of their polymer matrix composites. *Polymer Composites*, *25*, 470–479.

Bledzki, A. K., & Gassan, J. (1999). Composites reinforced with cellulose based fibres. *Progress in Polymer Science*, *24*, 221–274.

Dang, Z., Zhang, J., & Ragauskas, A. J. (2007). Characterizing TEMPO-mediated oxidation of ECF bleached softwood kraft pulps. *Carbohydrate Polymers*, *70*, 310–317.

De Nooy, A. E. J., Besemer, A. C., & van Bekkum, H. (1995). Selective oxidation of primary alcohols mediated by nitroxyl radical in aqueous solution. Kinetics and mechanism. *Tetrahedron*, *51*, 8023–8032.

Duanmu, J., Gamstedt, E. K., & Rosling, A. (2007). Hygromechanical properties of composites of crosslinked allylglycidyl-ether modified starch reinforced by wood fibres. *Composites Science and Technology*, *67*, 3090–3097.

Elazzouzi-Hafraoui, S., Nishiyama, Y., Putaux, J. L., Heux, L., Dubreuil, F., & Rochas, C. (2008). The shape and size distribution of crystalline nanoparticles prepared by acid hydrolysis of native cellulose. *Biomacromolecules*, *9*, 57–65.

Gandini, A. (2008). Polymers from renewable resources: A challenge for the future of macromolecular materials. *Macromolecules*, *41*, 9491–9504.

Gomez-Bujedo, S., Fleury, E., & Vignon, M. R. (2004). Preparation of cellouronic acids and partially acetylated cellouronic acids by TEMPO/NaClO oxidation of water-soluble cellulose acetate. *Biomacromolecules*, *5*, 565–571.

González-Sánchez, C., González-Quesada, M., De La Orden, M. U., & Urreaga, J. M. (2008). Comparison of the effects of polyethylenimine and maleated polypropylene coupling agents on the properties of cellulose-reinforced polypropylene composites. *Journal of Applied Polymer Science*, *110*, 2555–2562.

Goussé, C., Chanzy, H., Cerrada, M. L., & Fleury, E. (2004). Surface silylation of cellulose microfibrils: Preparation and rheological properties. *Polymer*, *45*, 1569–1575.

Habibi, Y., Chanzy, H., & Vignon, M. R. (2006). TEMPO-mediated surface oxidation of cellulose whiskers. *Cellulose*, *13*, 679–687.

Han, Y., Law, K.-N., Daneault, C., & Lanouette, R. (2008). Chemical and mechanical techniques for improving the papermaking properties of jack pine TMP fibers. *Tappi Journal*, *7*, 13–18.

Kaddami, H., Dufresne, A., Khelifi, B., Bendahou, A., Taourirte, M., Raihane, M., et al. (2006). Short palm tree fibers—Thermoset matrices composites. *Composites Part A—Applied Science and Manufacturing*, *37*, 1413–1422.

Levenspiel, O. (1972). *Fluid-particle Reactions in Chemical Reaction Engineering*. Oregon State University., pp. 357–373

Li, Z., Renneckar, S., & Barone, J. R. (2010). Nanocomposites prepared by in situ enzymatic polymerization of phenol with TEMPO-oxidized nanocellulose. *Cellulose*, *17*, 57–68.

Mao, L., Law, K.-N., Daneault, C., & Brouillette, F. (2008). Effects of carboxyl content on the characteristics of TMP fibers. *Industrial & Engineering Chemistry Research*, *47*, 3809–3812.

Mao, L., Ma, P., Law, K., Daneault, C., & Brouillette, F. (2010). Studies on kinetics and reuse of spent liquor in the TEMPO-mediated selective oxidation of mechanical pulp. *Industrial & Engineering Chemistry Research*, *49*, 113–116.

Martins, M. A., Forato, L. A., Mattoso, L. H. C., & Colnago, L. A. (2006). A solid state ^{13}C high resolution NMR study of raw and chemically treated sisal fibers. *Carbohydrate Polymers*, *64*, 127–133.

Mishra, S., Mohanty, A. K., Drzal, L. T., Misra, M., & Hinrichsen, G. (2004). A review on pineapple leaf fibers, sisal fibers and their biocomposites. *Macromolecular Materials and Engineering*, *289*, 955–974.

Montanari, S., Roumani, M., Heux, L., & Vignon, M. R. (2005). Topochemistry of carboxylated cellulose nanocrystals resulting from TEMPO-mediated oxidation. *Macromolecules*, *38*, 1665–1671.

Okita, Y., Saito, T., & Isogai, A. (2009). TEMPO-mediated oxidation of softwood thermomechanical pulp. *Holzforschung*, *63*, 529–535.

Okita, Y., Saito, T., & Isogai, A. (2010). Entire surface oxidation of various cellulose microfibrils by TEMPO-mediated oxidation. *Biomacromolecules*, *11*, 1696–1700.

Paunikallio, T., Suvanto, M., & Pakkanen, T. T. (2006). Viscose fiber/polyamide 12 composites: Novel gas-phase method for the modification of cellulose fibers with an aminosilane coupling agent. *Journal of Applied Polymer Science*, *102*, 4478–4483.

Reich, S., El Sabbagh, A., & Steuernagel, L. (2008). Improvement of fibre–matrix-adhesion of natural fibres by chemical treatment. *Macromolecular Symposia*, *262*, 170–181.

Saito, T., & Isogai, A. (2004). TEMPO-mediated oxidation of native cellulose. The effect of oxidation conditions on chemical and crystal structures of the water-insoluble fractions. *Biomacromolecules*, *5*, 1983–1989.

Saito, T., Shibata, I., Isogai, A., Suguri, N., & Sumikawa, N. (2005). Distribution of carboxylate groups introduced into cotton linters by the TEMPO-mediated oxidation. *Carbohydrate Polymers*, *61*, 414–419.

Saito, T., Hirota, M., Tamura, N., Kimura, S., Fukuzumi, H., Heux, L., et al. (2009). Individualization of nano-sized plant cellulose fibrils by direct surface carboxylation using TEMPO catalyst under neutral conditions. *Biomacromolecules*, *10*, 1992–1996.

Sbiai, A., Maazouz, A., Fleury, E., Sautereau, H., & Kaddami, H. (2010). Short date palm tree fibers/polyepoxy composites prepared using RTM process: Effect of Tempo-mediated oxidation of the fibers. *BioResources*, *5*, 672–689.

Segal, L., Creely, J. J., Martin, A. E., & Conrad, C. M. (1959). An empirical method for estimating the degree of crystallinity of native cellulose using the X-ray diffractometer. *Textile Research Journal*, *29*, 786–794.

Shibata, I., & Isogai, A. (2003). Depolymerization of cellouronic acid during TEMPO-mediated oxidation. *Cellulose*, *10*, 151–158.

Wikberg, H., & Maunu, S. L. (2004). Characterisation of thermally modified hard and softwoods by ^{13}C CPMAS NMR. *Carbohydrate Polymers*, *58*, 461–466.

Zimmermann, T., Pöhler, E., & Geiger, T. (2004). Cellulose fibrils for polymer reinforcement. *Advanced Engineering Materials*, *6*, 754–761.